Evaluation of DNA-binding, cleavage, BSA interaction of Zn-hydroxy flavone complex

S. Iyyam Pillai[a], K. Vijayaraghavan[a] and S. Subramanian[b]*

[a]Department of Chemistry, Pachaiyappa's College, Chennai, Tamilnadu, India.
[b]Department of Biochemistry, University of Madras, Guindy Campus, Chennai, Tamilnadu, India

_____

ABSTRACT

Zinc is an essential trace element vital for many physiological functions. In the present study, DNA binding and cleavage activities of a novel Zn-flavonol complex was investigated. The interaction of the complex with CT-DNA has been explored by absorption, emission, viscosity and circular dichoric measurements. The complex exhibited hypochromicity in absorption and an increase in specific viscosity, which revealed that the complex bound to CT-DNA through an intercalation mode. The calculated intrinsic binding constant (K_b) was found to be 6.2 x 10^4 M^{-1}. The data revealed that the complex facilitates the cleavage of super coiled pBR322 DNA (Form I) to the open circular form (Form II) and linear form (Form III) via a hydrolytic pathway. Further, the synthesized complexes altered the intrinsic fluorescence of bovine serum albumin (BSA) through a static quenching with the binding constants (K_{sv}) of 1.6 x 10^5 M^{-1} with a number of binding sites of 0.98.

Keywords: Zn-hydroxy flavone; DNA binding and cleavage; hydrolytic cleavage; Intercalation mode; BSA binding.

Abbreviations

DNA	Deoxyribose nucleic acid
CT	Calf Thymus DNA
DMSO	Dimethyl Sulphoxide
BSA	Bovine Serum Albumin
Zn	Zinc
Tris-HCl	Tris(hydroxymethyl)aminomethane
EB	Ethidium Bromide
KI	Pottassium Iodide
NaN_3	Sodium azide
SOD	Super oxide Dismutase
EDTA	Ethylenediaminetetraacetic acid

_____

INTRODUCTION

Discoveries in the field of inorganic and bio-inorganic chemistry pose a significant impact on modern clinical medicine. These discoveries have predominantly emerged in the form of either metal-containing diagnostic imaging agents or metal-containing therapeutics [1]. Ever since the landmark discovery of cisplatin, an archetypal inorganic drug, as a DNA reactive therapeutic agent, much efforts have been devoted to the development of novel platinum drugs and elucidation of cellular responses to them to alleviate the dose limiting side effects associated with cisplatin in clinical use. These problems have also prompted chemists to develop alternative strategies using various metals and aimed at different targets [2]. The ability of metal complexes to form structures with unique and defined shapes suggests that it is worth exploring a different aspect of metal complexes. However, transition metals appear especially appealing for this purpose because they can support a multitude of coordination numbers and geometries that go beyond the linear, trigonal planar and tetrahedral binding geometries of carbon.

379

_____

Zn is a star player in bioinorganic chemistry [3]. Zn is second abundant essential transition metal ion in humans succeeding Fe. It has diverse physiological functions. Recently, DNA binding proteins that use Zn to organize structural elements, called Zn fingers, have been elucidated [4]. Zn is attractive because of its redox-inertness and wide repertoire of co-ordinate ligands, sequestration of other metal ions by special protein-drug complexes is a further possibility [5].

Flavonoids, as part of the human diet, are a group of polyphenolic phytochemicals that have multiple biological effects as antioxidants, antiviral and antimutagenic agents [6-8]. They have a basic structure of 2-phenyl-benzo-c-pyrones. Furthermore, flavonoids are effective metal ion chelators [9-12]. The experimental and theoretical studies have shown that the ideal complexation site for flavonoids involves the hydroxyl group on carbon 3 or 5 and the adjacent 4-carbonyl group. As the transition metal ions play a vital role in initiation of free radical processes (via Fenton reaction) metal ion chelation is widely considered as another mechanism for the antioxidant activity of flavonoids. At the same time, the interaction of flavonoids with metal ions may alter antiradical properties and some of the biological effects of the flavonoids [13].

DNA is the primary intracellular target of most anticancer and antiviral therapies according to cell biology [14]. The phosphate diesters are known to serve as nucleotide linkages in the genetic DNA. Phosphate diesters are exceptionally stable, making them uniquely suited to their role as the backbone for genetic material. Typical nucleases accelerate the rate of DNA hydrolysis by factors exceeding 10^{10} [15].

The mechanism of DNA-binding and behavior of the metal complexes as novel cancer therapeutic agents are strongly attributed to the size, shape, and planarity of the intercalative ligands. It is also known that metal complexes may interact with DNA either covalently or non-covalently. In covalent binding, the labile part of the complexes is replaced by a nitrogen base of DNA such as guanine *via* its N7 donor atom. On the other hand, the non-covalent DNA interactions include intercalative, electrostatic and groove binding of cationic metal complexes along outside of DNA helix, the major or minor groove. Intercalation involves the partial insertion of aromatic heterocyclic rings between the DNA base pairs. The complexes binds to DNA through interstrand cross-linkage between neighboring guanine residues bound covalently through purine nitrogen atoms, thus affecting replication, transcription and DNA repair [16]. Generally, DNA cleavage follows an oxidative or hydrolytic cleavage pathway. The hydrolytic pathway proceeds through hydrolysis of the phosphodiester bond, leading to fragmentation of DNA and such pathways are mediated by enzymatic process, while the oxidative process involves the oxidation of nucleobases and/or H^+ abstraction from the sugar moiety.

The investigation of compounds with respect to their binding to albumins becomes important because of the pharmacokinetic and pharmacodynamics role of such binding [17,18]. Serum albumins are most abundant proteins in the circulatory system of a wide variety of organisms. They have important role in bioregulatory functions like maintenance of the colloidal osmotic blood pressure and blood pH. In addition, serum albumins serve as depot proteins and as transport proteins for a variety of endogenous and exogenous substances such as fatty acids, hormones and drugs [19-21]. In general, bovine serum albumin (BSA) has been extensively used because of its structural homology with human serum albumin (HSA) [22,23]. BSA is the most abundant protein of plasma and has been widely used a model system to study protein aggregation and for biotechnological folding, application. BSA is a well-known protein which displays tendency to self-assembly in large macromolecular aggregates under a variety of conditions [24,25]. Therefore, it is always chosen as a relevant protein and has become the best-studied model of general drug-protein interactions [23].

The present work stems from our interest to investigate the binding mode of DNA and nuclease activity of the hydroxy flavone Zn(II) complex [26]. The possible structure model of the complex is shown Figure 1. The mechanistic investigation demonstrated that hydroxy flavone Zn(II) complex bound to DNA *via* intercalation mode and promotes cleavage *via* hydrolytic pathway.

_____
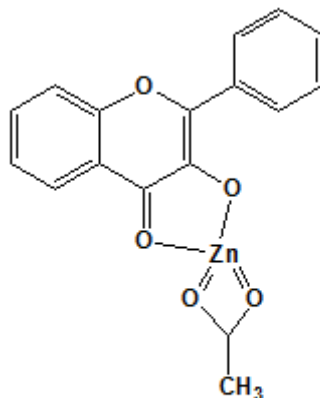
Figure 1

Figure 1. The possible structure model of the complex

MATERIALS AND METHODS

2.1 Materials and instrumentation

UV–Visible spectra were recorded using Perkin Elmer Lambda 35 spectrophotometer operating in the range of 200–500 nm with quartz cells and ε values are expressed in M^{-1} cm^{-1}. The emission spectra were recorded on a Perkin Elmer LS-45 fluorescence spectrometer. Viscosity measurements were recorded using a Brookfield Programmable LV DVII+ viscometer. Tris(hydroxymethyl)aminomethane–HCl (Tris–HCl) buffer solution was prepared using deionized and sonicated triple distilled water. The supercoiled pBR322 DNA and Calf thymus (CT) DNA were procured from Bangalore Genie (India). Circular dichoric spectra of CT-DNA were obtained using a JASCO J-715 spectropolarimeter equipped with a Peltier temperature control device at $25 \pm 0.1°C$ with 0.1 cm path length cuvette.

2.2 DNA binding experiments

2.2.1. Absorption spectral studies

Electronic absorption spectrum of the complex was recorded before and after addition of CT-DNA in the presence of 50 mM Tris-HCl buffer (pH 7.5). A fixed concentration of metal complexes (10 µM) was titrated with incremental amounts of CT-DNA over the range (0 – 200 µM). The equilibrium binding constant (K_b) values for the interaction of the complex with CT-DNA were obtained from absorption spectral titration data using the following equation 1 [27].

$$[DNA]/ (\varepsilon_a - \varepsilon_f) = [DNA]/ (\varepsilon_b - \varepsilon_f) + 1/K_b (\varepsilon_b - \varepsilon_f) \tag{1}$$

Where ε_a is the extinction coefficient observed for the charge transfer absorption at a given DNA concentration, ε_f the extinction coefficient at the complex free in solution, ε_b the extinction coefficient of the complex when fully bound to DNA, K_b the equilibrium binding constant, and [DNA] the concentration in nucleotides. A plot of [DNA]/ $(\varepsilon_a - \varepsilon_f)$ versus [DNA] gives K_b as the ratio of the slope to the intercept. The non-linear least square analysis was performed using Origin lab, version 6.1.

2.2.2. Fluorescence spectral studies

Experiments were carried out at pH 7.2 in the buffer containing Tris – HCl buffer 50 mM by keeping EB-DNA solution containing [EB] = 4µM and [DNA] = 50 µM as constant and varying the concentration of complex (0 - 100 µM). Fluorescence spectra were recorded using excitation wavelength of 496 nm and the emission range set between 550 and 750 nm. The quenching constant K_{sv} was deduced from Stern-Volmer method where the ratio of fluorescence of the compound alone (I_0) over the fluorescence of the compound in the presence of CT-DNA (I) is presented as a function of CT-DNA concentration.

$$I_o/I = 1 + K_{sv} [r]. \tag{2}$$

Where I_0, is the ratio of fluorescence intensities of the complex alone, I is the ratio of fluorescence intensities of the complex in the presence of CT-DNA. K_{sv} is a linear Stern – Volmer quenching constant and r is the ratio of the total concentration of quencher to that of DNA, [M] / [DNA]. A plot of I_0 / I *vs.* [complex]/ [DNA], K_{sv} is given by the

_____

ratio of the slope to the intercept. The apparent binding constant (K_{app}) was calculated using the equation $K_{EB}[EB] / K_{app}[complex]$, where the complex concentration was the value at a 50% reduction of the fluorescence intensity of EB and $K_{EB} = 1.0 \times 10^7$ M^{-1} ([EB] = 3.3 µM) [28].

2.2.3. Viscosity measurements
The binding mode of the complex to CT-DNA, viscosity measurements were carried out on CT-DNA (0.5 mM) by varying the concentration of the complex (0.01 mM, 0.02 mM, 0.03 mM, 0.04 mM, 0.05 mM). Data were presented as (η/η_o) versus binding ratio of concentration of complex to that of concentration of CT-DNA , where η is the viscosity of DNA in the presence of complex and η_o is the viscosity of DNA alone.

2.2.4. Circular dichoric spectral studies
Incubation of the DNA with the Zn(II) complex induced notable changes in CD spectrum. The spectrum were recorded in the region of 220-320 nm for 200 µM DNA in the presence of 100 µM of Zn-flavonol complex.

2.2.5. Protein binding studies
Fluorescence spectra were recorded from 300 to 500 nm with the excitation wavelength at 280 nm. First 3 ml of solution containing an appropriate concentration (~1 µmol/L) of BSA was titrated by the successive addition of complex solution. Titrations were executed in the absence and the presence of the complex in the room temperature with incubation period of 5 min. Under strictly controlled temperature and pH value, the cause of fluorescence quenching mode is, as below, dynamic or static quenching. In order to determine the quenching property, the fluorescence decay data were analyzed *via* the Stern-Volmer equation [29]:

$$F_0 / F = 1 + K_{sv} [Q] \tag{3}$$

Where F_0 and F are the steady-state fluorescence intensities in the absence and the presence of quencher, respectively. K_{sv} is the Stern-Volmer quenching constant and [Q] is the concentration of quencher. The plot of F_0 / F vs [Q] shows the value of K_{SV}. According to the equation (4):

$$K_{SV} = K_q \tau_0 \tag{4}$$

where K_q is the quenching rate constant and τ_0 is the fluorescence life time of protein in the absence of quencher, the value of τ_0 is considered to be 10^{-8} s.

When small molecules bind independently to a set of equivalent sites on a macromolecule, the equilibrium between free and bound molecules is given by the following equation [30].

$$Log(F_0 - F)/F = logK + nlog[Q] \tag{5}$$

Where K is the binding constant to a site and n is the number of binding sites per BSA. The binding constant K and the number of binding sites n can be obtained by using equation. (5).

The absorption titrations of BSA in the presence and the absence of complex were implemented in the range of 200 - 500 nm. BSA concentrations were fixed at 10 µmol/L. The influence of the absorbance of complexes was reduced by adding in the reference cells the solutions of complexes of the same concentrations as in the sample solution.

2.3. DNA cleavage experiments
The DNA cleavage experiments were performed by agarose gel electrophoresis. pBR322 DNA (0.1µg/µl) in Tris-buffer (pH 7.2) was treated with complex (50 µM) in the presence of additives. The sample was incubated for 3h at 37ºC and the reaction was quenched by 1 µl of loading buffer. pBR322 DNA bands were stained by EB, visualized under UV light and photographed. The extent of cleavage of SC DNA was determined by measuring the intensities of the bands using a UVITECH Gel Documentation System.

RESULTS

3.1. DNA binding experiments
3.1.1. Absorption spectral studies
The binding of Zn-hydroxy flavone complex to CT-DNA was monitored classically through absorption titration method. The absorption spectra of the complex in the presence and absence of CT-DNA is shown in Figure 2. Metal complex bound to DNA through intercalation is characterized by change in the absorbance (hypochromism) and red

_____

shift in wavelength, due to the intercalative binding mode involving a stacking interaction between the DNA base pairs.
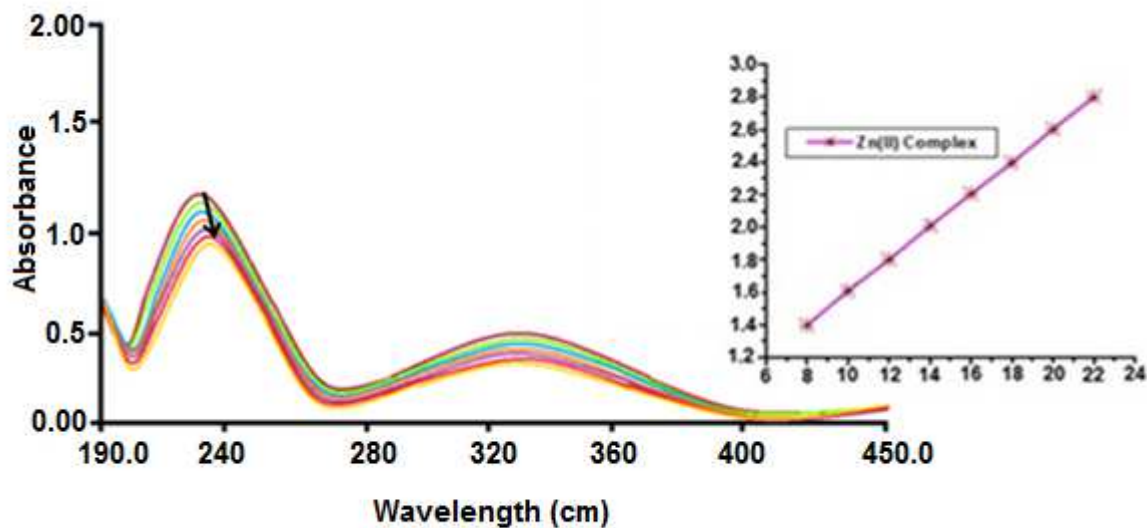
Figure 2

Figure 2. Absorption spectra of the complex (25 µM) in the absence and presence of increasing amounts of CT-DNA (0 - 200 µM) in Tris-HCl buffer. Insets: Plot of [DNA]/($\varepsilon_a - \varepsilon_f$) vs [DNA] for absorption titration of CT-DNA and complex

3.1.2. Fluorescence spectral studies

The complex emits prominent luminescence in Tris-buffer with a maximum emission wavelength of about 350 nm. The well-behaved titration of the complex with CT-DNA is displayed in Figure 3. On addition of CT-DNA to the complex, enhancement in fluorescence without wavelength shift was observed in the region of 340-360 nm.
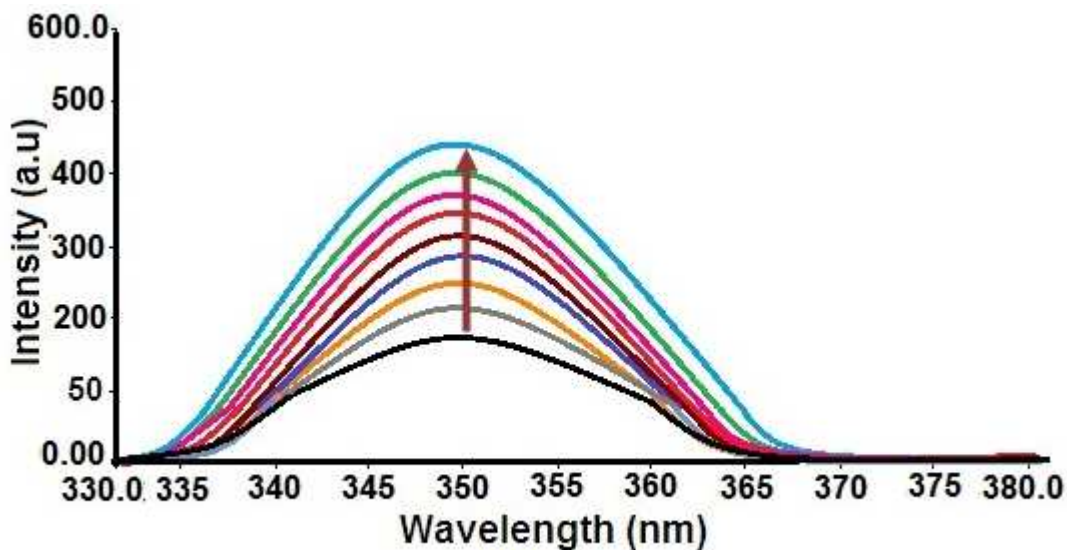
Figure 3

Figure 3. The change of emission fluorescence spectra of vanadium complex (25 µM) in the absence and presence of increasing amounts of CT-DNA. The arrow shows the intensity increased with increasing amounts of DNA

Steady state competitive binding experiments using the Zn-hydroxy flavone as quenchers were undertaken to get further proof for the binding of the compounds to DNA via intercalation. EB emits intense fluorescence at about 620 nm in the presence of DNA due to its strong intercalation with adjacent DNA base pairs. The relative binding of EB bound to DNA in the absence and presence of complex using emission spectra are given in Figure 4. The emission band at 618 nm of the DNA-EB moiety decreased in intensity upon increasing the complex concentration.

_____
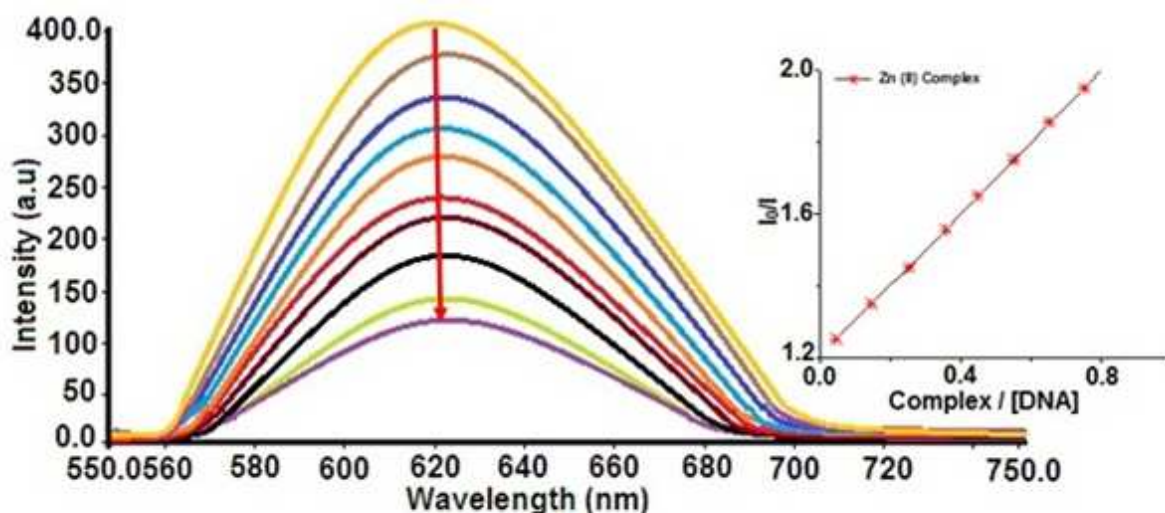
Figure 4

Figure 4. Emission spectra of EB bound to DNA in Tris – HCl buffer (pH 7.2) in the absence and presence of the complex. [EB] = 4 µM, [DNA] = 40 µM, [complex] = 0 to 100 µM. (λ_{ex} = 480 nm). The arrow shows the intensity changes on increasing the complex concentration. The inset shows the plot of I_0/I vs. [complex]/ [DNA] for fluorescence quenching curves of EB-DNA by complex

3.1.3. Viscosity measurements studies

For further clarifying the binding of the complex with CT-DNA, viscosity studies were carried out. The results of the viscosity measurements are represented in   Figure 5.
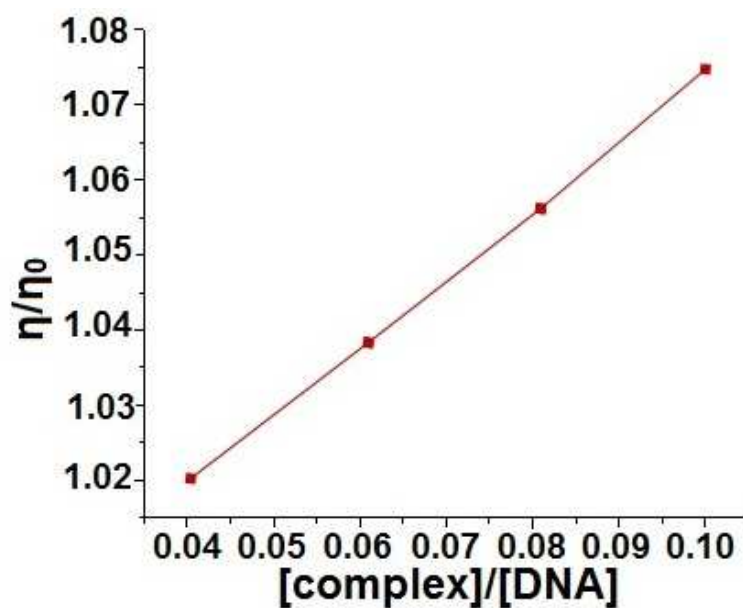
Figure 5

Figure 5. Changes in relative viscosity of CT-DNA on increasing amounts of complex

3.1.4. Circular dichoric spectral studies

Upon the addition of the complex to CT-DNA, the CD spectrum undergoes changes in both positive and negative bands in intensity as represented in Figure 6.

384

_____
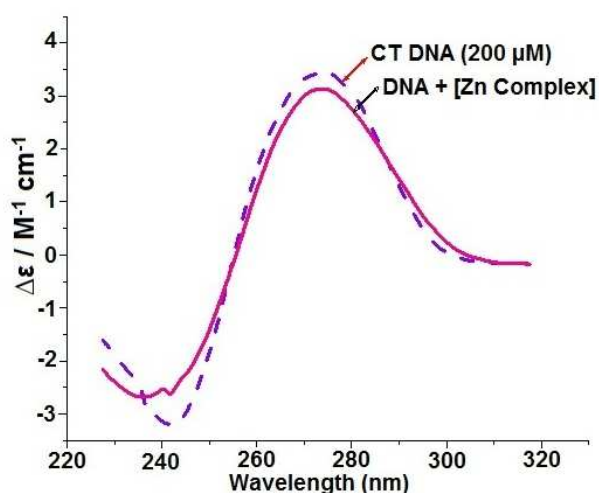
Figure 6

Figure 6. CD spectra was recorded over the wavelength range 220-320 nm of CT-DNA and the complex

3.2. DNA cleavage experiments

Figure 7 and Figure 8 shows agarose gel electrophoresis patterns for the cleavage of plasmid DNA after being induced by increasing the concentrations of the complex and Zn(II) salt under the same experimental conditions in the absence of external agents. The conversion of supercoiled DNA to the nicked DNA and linear DNA becomes more efficient when increasing the concentration of the complex. As shown Figure 9, no evident inhibition of DNA cleavage activity was observed in the presence DMSO (lane 3), KI (lane 4), NaN_3 (lane 6), L -histidine (lane 7) and SOD (lane 8), which suggests that, the DNA cleavage activity of the complex might not occur *via* an oxidative pathway rather *via* a hydrolytic and/or interaction.
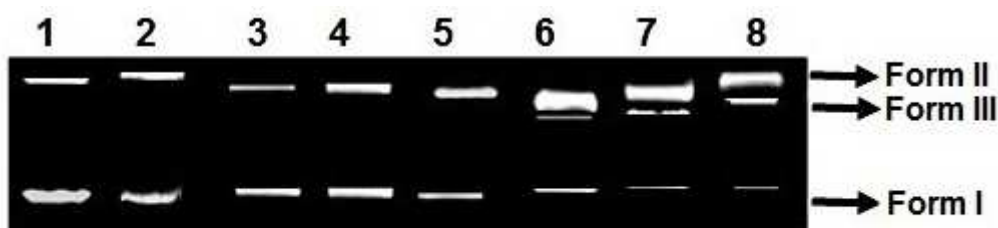
Figure 7

Figure 7. Cleavage of plasmid pBR322 DNA (50 µM) with varying concentration of complexes at 37ºC in Tris – HCl buffer (pH 7.2). Lane 1, DNA control; Lanes 2-8: DNA + Complex (10, 20, 30, 40 50, 75 and 100 µM: incubation for 3 h)
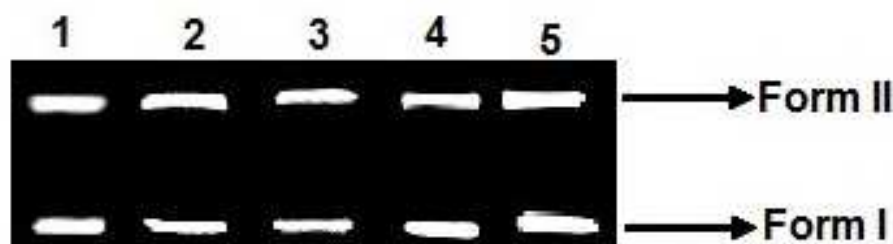
Figure 8

Figure 8. Cleavage of plasmid pBR322 DNA (50 µM) with Zn(II) acetate at 37ºC in Tris – HCl buffer (pH 7.2). Lane 1, DNA control; Lane 2-5: DNA + Zn(II) acetate. [10, 25, 50 and 100 µM incubation for 3 h]

_____
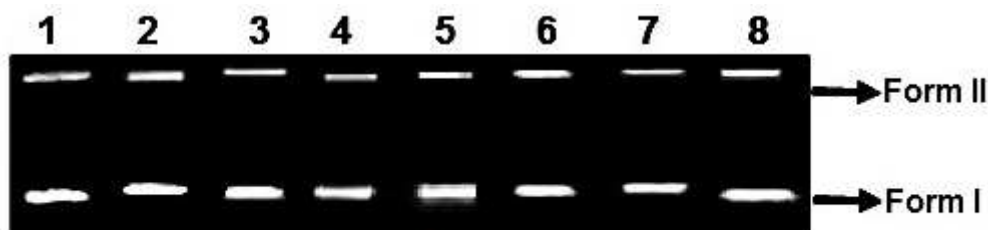
Figure 9. Gel electrophoresis diagrams showing the cleavage of pBR322 DNA (50 µM) by complex in presence of different additives at pH 7.2 and 37ºC; Lane 1: DNA control; Lane 2: DNA + complex; Lanes 3-8: DNA + complex (50 µM) + (DMSO, KI, EDTA, NaN₃, L-histidine and SOD)

3.3. Protein Binding studies
3.3.1. Fluorescence quenching of BSA by complex

BSA solutions exhibit a strong fluorescence emission with a peak at 348 nm when excited at 285 nm. Under the same experimental condition, the emission intensities of the complex were very weak. Figure 10, shows the result of increasing the concentration of complex on the fluorescence emission of BSA. The intensity of characteristic emission band at 348 nm decreased gradually with the increasing concentration of the metal complex without any shift, which validate that, the interaction between metal complexes and BSA have occurred.
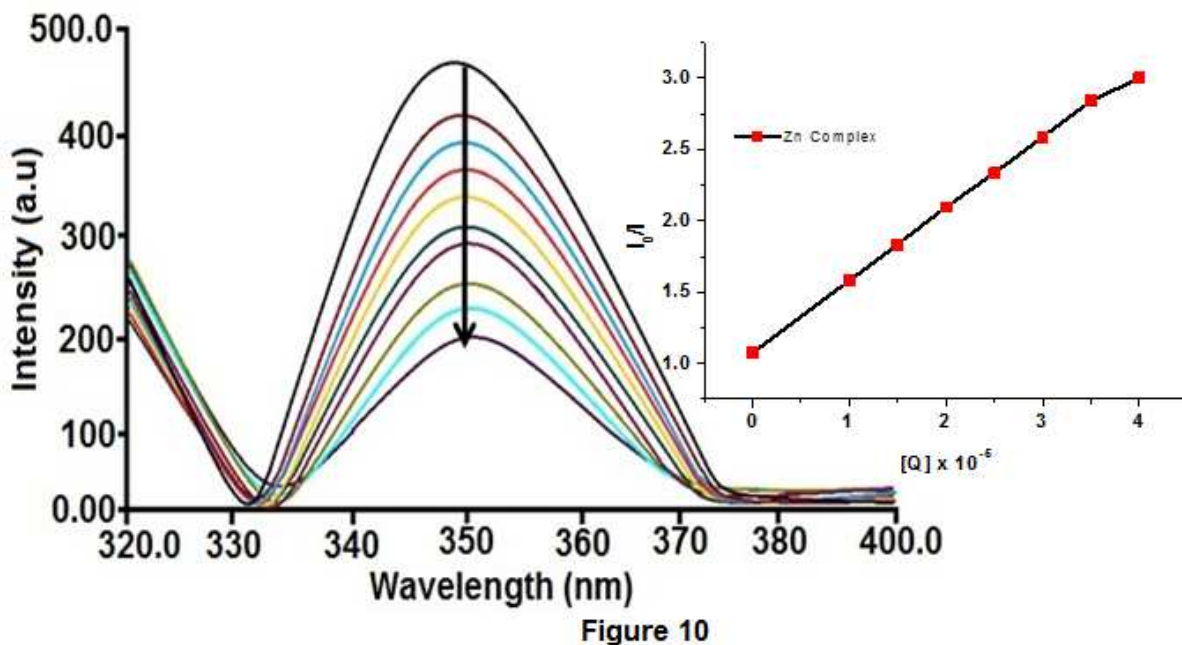
Figure 10. Fluorescence spectra of BSA in presence of various concentration of complex [BSA] = 1.0×10^{-6} molL^{-1}. Inset shows the plots of emission intensity I_o / I vs [Q]. [Q = complex]

3.3.2. UV-visible spectral absorption spectral analysis

The representative absorption spectrum of free BSA and BSA-complex is depicted in Figure 11. The absorption band obtained for BSA at 280 nm in the absence of metal complexes showed an increase in the intensity of absorption after the addition of complex.

386

_____
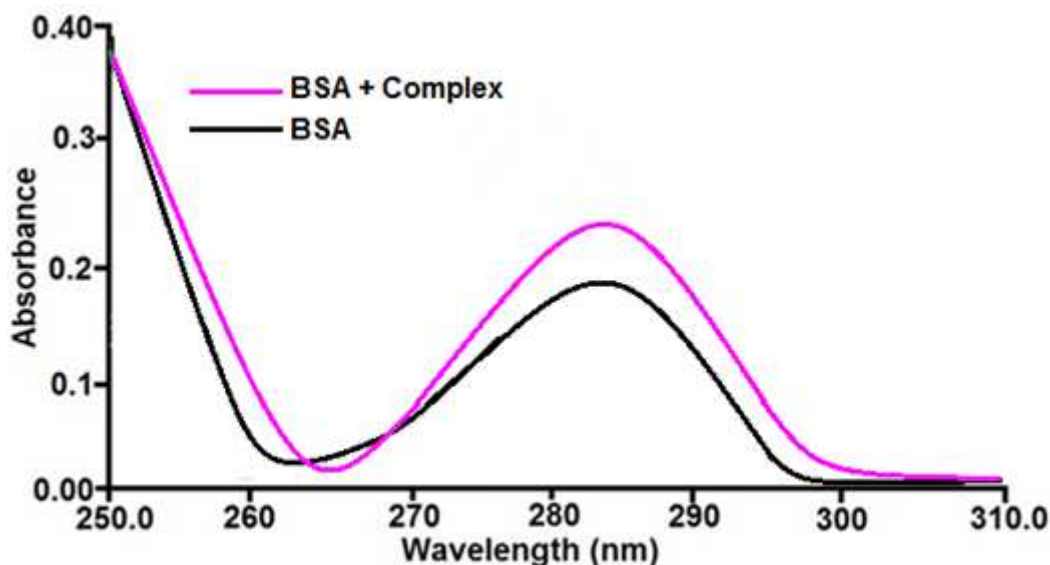
Figure 11

Figure 11. Absorption spectra of BSA in presence of various concentration of complex Vs [BSA] [complex] = 10×10^{-6} molL^{-1}

DISCUSSION

DNA binding is the critical step for DNA cleavage in most cases. Therefore, the binding ability of the complex to CT-DNA was studied by using UV-Vis absorption spectroscopy. Upon addition of increasing concentration of CT-DNA (0 – 200 μM) a significant ''hypochromic'' effect in the intraligand bands at 220– 240 nm was observed accompanied by a strong red shift of 6-8 nm, an indicative of stabilization of the DNA helix. The hypochromicity suggests the complex may bind to DNA by intercalation mode, due to a strong interaction between the electronic states of the intercalating chromophore and those of the DNA bases [31]. These observations can be rationalized by the following reasons. When the complex intercalates the base pairs of DNA, the Π^*- orbital of the intercalated ligand in the complex can couple with the Π orbital of the DNA base pairs, thus decreasing the Π^*- Π transition energy resulting in the bathochromism. Furthermore, the coupling Π – orbital is partially filled by electrons, thus decreasing the transition probabilities and concomitantly resulting in hypochromism [32]. The intrinsic binding constant (K_b) of the complex to CT-DNA have been calculated to quantify the extent of DNA binding. The binding constant of the complex was determined to be 6.2 x 10^4 M^{-1}. To further confirm the interactions between the studied complex and CT-DNA, emission experiments were carried out. The result revealed that the stronger enhancement of fluorescence intensity for the complex may be largely due to the interaction between the adjacent base pairs of the CT-DNA and the complex. The observed result agrees with those of other intercalators [33-35]. To clarify the interaction pattern of the complex with CT-DNA, a fluorimetric competitive binding experiment was carried out using ethidium bromide (EB) as a host, which shows no apparent emission intensity in buffer solution due to the solvent quenching. It has been reported that the enhanced fluorescence emission intensity can be quenched by the addition of another molecule [36]. Fluorescence intensities at 618 nm were measured at different complex concentrations. The emission band at 618 nm of the DNA-EB moiety decreased in intensity upon increasing the complex concentration. The apparent binding constants (K_{app}) at room temperature were calculated to be 5.3 x 10^5M^{-1}. Viscosity, sensitive to length increase is regarded as the one of the least ambiguous and the most relevant tests of binding model with CT-DNA in solution in the absence of crystallographic structural data [37]. On increasing the amount of the complex, the relative viscosity of DNA increases steadily. The viscosity experimental results thus provide strong evidence for the interaction of the complex with CT-DNA by intercalation mode. Circular dichoric spectral investigation is useful in monitoring the conformational variations of DNA during complex-DNA interactions [38]. The CD spectrum of CT-DNA exhibits a positive band at 275 nm due to base stacking and a negative band at 245 nm due to helicity of B-type DNA [39]. The decrease in ellipticity is due to the destabilization of DNA form attributed to the opening of DNA structure by the formation of intra-strand DNA cross-linkings. The decrease in both the bands suggests that the complex can unwind the DNA helix and lead to loss of helicity.

In order to evaluate the function of the complex to incise pBR322 DNA, the cleavage reaction of supercoiled pBR322 was monitored by agarose gel electrophoresis. Figure 7. Form I Plasmid DNA is gradually converted in to Form II (Lanes 2-5). Form III began to appear in the presence of 50 μM and above (Lanes 6-8). However, no cleavage activity was observed in the control experiments with Zn(II) salt as depicted in Figure 8. These results revealed that the Zn(II) salt did not show DNA cleavage activity but the Zn flavonol complex play a vital role in

387

_____

DNA cleavage, and the degradation activity of the complex is obviously concentration dependant. In order to further clarify the DNA cleavage mechanism promoted by complex, hydroxyl radical scavenger (DMSO and KI) and singlet oxygen scavenger (NaN$_3$ and L-histidine), superoxide quenchers (superoxide dismutase enzyme SOD) and chelating agent (EDTA) were introduced in the incubation mixture as shown in Figure 9. The EDTA a chelating agent that strongly binds to Zn(II) (lane 5) forming a stable complex, can efficiently inhibit DNA cleavage, indicating Zn(II) complex play the key role in the DNA cleavage activity.

Generally, the fluorescence of a protein is caused by three intrinsic characteristics of the protein, namely tyrosine, tryptophan and phenylalanine residues. In fact, the intrinsic fluorescence of many proteins is mainly contributed by tryptophan alone. However, due to very low quantum yield of phenylalanine, fluorescence of a tyrosine is almost completely quenched if that tyrosine is ionized [40]. Quenching can be classified as either dynamic or static quenching by different mechanism. Dynamic quenching results from collision between fluorophore and quencher, and static quenching is due to the formation of ground-state complex between fluorophore and quencher. In general, dynamic and static quenching can be distinguished by their different dependences on temperature and viscosity. The quenching rate constants decrease with increase in temperature for static quenching, but the reverse effect is observed for dynamic quenching [41]. The value of n is found to be 0.98. The values of n is basically associated with binding constants, which implies a direct relation between the binding constant and number of binding sites. The binding constant value of the synthesized complex was found to 1.6 x 10^5 M^{-1}. The K$_{sv}$ value (10^5 M^{-1}) of the metal complex is higher than the maximum scatter collision-quenching constant of diverse kinds of quenchers for biopolymers fluorescence (2 x 10^4 M^{-1}S^{-1}) indicating the existence of static quenching mechanism. UV-visible absorption investigation is a very simple and effective method in exploring the structural change and detecting the complex formation [42]. From the Figure 11, we can reveal that there exists a static interaction between BSA and the respective complex of due to the formation of ground state complex of the type BSA-complex as reported earlier [43].

In summary, the binding interaction between the Zn flavonol complex and CT-DNA has been sustained by using UV-Visible, fluorescence, viscosity and circular dichroic measurements. The obtained results collectively showed that the Zn complex binds to CT-DNA by an intercalating mode. The complex exhibited strong nuclease activity in the absence of any oxidizing and reducing agents. Future clinical success will benefit from targets through interdisciplinary collaboration, which are highly specific for cancer cells.

<div align="center">

REFERENCES

</div>

[1] C. Orvig, M. J. Abrams, Chem Rev., 99, **1999,** 2201-2204.
[2] P. C. Bruijnincx, P. J. Sadler, *Chem. Biol.*, 12, **2008,** 197-206.
[3] S. J. Lippard, J. M. Berg, In Principles of Bioinorganic Chemistry, University Science, Books, Mill Valley, California, **1994**.
[4] O. Leon, M. Roth, *Biol. Res.,* 33, **2000,** 21-30.
[5] K. D. Karlin, *Science,* 261, **1993**, 701-708.
[6] P. Cos, L. Ying, M. Calomme, J. P. Hu, K. Cimanga, B. Van Poel, L. Pieters, A. J. Vlietinck, D. Vanden Berghe, *J. Nat. Prod.,* 61, **1998,** 71-76.
[7] D. A. R. Vanden Berghe, A. Haemers, A. J. Vlietinck, CRC Press, Boca Raton, **1993,** 405-440.
[8] W. Bors, W. Heller, C. Michel, M. Saran, *Methods Enzymol.,* 186, **1990,** 343-355.
[9] E. Jr. Middleton, C. Kandaswami, T. C. Theoharides, *Pharmacol. Rev.,* 52, **2000,** 673-751.
[10] M. Thompson, C. R. Williams, G. E. Elliot, Anal. *Chim. Acta.,* 85, **1976,** 375-381.
[11] A. C. Boudet, J. P. Cornard, J. C. Merlin, *Spectrochim. Acta., A. Mol. Biomol. Spectrosc.*, 56, **2000,** 829-839.
[12] M. T. Fernandez, M. L. Mira, M. H. Florêncio, K. R. Jennings, *J. Inorg. Biochem.,* 92, **2002,** 105-111.
[13] G. Dehghan, J. E. Dolatabadi, A. Jouyban, K. A. Zeynali, S. M. Ahmadi, S. Kashanian, *DNA and Cell Biol.*, 30, **2011**, 195-201.
[14] K. Jiao, Q. X. Wang, W. Sun, F. F. Jian, *J. Inorg. Biochem.,* 99, **2005,** 1369-1375.
[15] E. H. Serpersu, D. Shortle, A. S. Mildvan, *Biochemistry,* 26, **1987,** 1289-1300.
[16] C. P. Saris, P. J. van de Vaart, R. C. Rietbroek, F. A. Blommaert, *Carcinogenesis*, 17, 1996**,** 2763-2769.
[17] E. G. Ferrer, A. Bosch, O. Yantorno, E. J. Baran, *Bioorg. Med. Chem.*, 16, **2008,** 3878–3886.
[18] N. M. Urquiza, L. G. Naso, S. G. Manca, L. Lezama, T. Rojo, P. A. M. Williams, E. G. Ferrer, *Polyhedron*, 31, **2012,** 530-538.
[19] D. C. Carter, J. X. Ho, *Adv. Protein Chem.*, 45, **1994**, 153-203.
[20] T. Peter, All about Albumin: Biochemistry, Genetics, and Medical Applications, Academic Press, NewYork, **1996**.
[21] G. Vignesh, S. Arunachalam, S. Vignesh, R. A. James, *Spectrochim. Acta. A. Mol. Biomol. Spectrosc.*, 96, **2012,** 108-116.

_____

[22] K. S. Ghosh, S. Sen, B. K. Sahoo, S. Dasgupta, *Biopolymers,* 91, **2009**, 737-744.

[23] P. Sathyadevi, P. Krishnamoorthy, E. Jayanthi, R. R. Butorac, A. H. Cowley, N. Dharmaraj, *Inorganica. Chimica. Acta*., 384, **2012,** 83-96.

[24] V. Militello, C. Casarino, A. Emanuele, A. Giostra, F. Pullara, M. Leone, *Biophys. Chem.*, 107, **2004**, 175-187.

[25] G. Navarra, D. Giacomazza, M. Leone, F. Librizzi, V. Militello, P. L. San Biagio, *Eur. Biophys. J.,* 38, 2009, 437-446.

[26] K. Vijayaraghavan, S. Iyyam Pillai, S. P. Subramanian, *Eur. J. Pharmacol.,* 680, **2012,** 122-129.

[27] A. Wolf, G. H. Jr. Shimer, T. Meehan T, *Biochemistry*, 26, **1987,** 6392-6396.

[28] J. R. Lakowicz, G. Weber, *Biochemistry,* 12, **1973,** 4161-4170.

[29] J. R. Lakowicz, Principles of Fluorescence Spectroscopy, third ed., Plenum Press, New York, 2006.

[30] J. Min, X. Meng-Xia, Z. Dong, L. Yuan, L. Xiao-Yu, C. Xing, *J. Mol. Struct.*, 692, 2004, 71–80.

[31] S. Tabassum, A. Asim, F. Arjmand, M. Afzal, V. Bagchi, *Eur. J. Med. Chem.*, 58, **2012**, 308-316.

[32] S. Sobha, R. Mahalakshmi, N. Raman, *Spectrochim. Acta. A. Mol. Biomol. Spectrosc.,* 92, **2012,** 175-183.

[33] Y. M. Song, Q. Wu, P. J. Yang, N. N. Luan, L. F. Wang, Y. M. Liu, *J. Inorg. Biochem.,* 100, **2006,** 1685-1691.

[34] A. Silvestri, G. Barone, G. Ruisi, M. T. Lo Giudice, S. Tumminello, *J. Inorg. Biochem.,* 98, **2004**, 589-594.

[35] J. Tan, L. Zhu, B. Wang, *Dalton Trans.*, **2009,** 4722-4728.

[36] J. Qian, L. Wang, W. Gu, X. Liu, J. Tian, S. Yan, *Dalton Trans.*, 40, **2011,** 5617-5624.

[37] S. Satyanarayana, J. C. Dabrowiak, J. B. Chaires, *Biochemistry*, 32, **1993**, 2573-2584.

[38] A. M. Polyanichko, V. V. Andrushchenko, E. V. Chikhirzhina, V. I. Vorob'ev, H. Wieser, *Nucleic Acids Res.,* 32, **2004**, 989-996.

[39] A. Rajendran, B. U. Nair, *Biochim. Biophys. Acta.*, 1760, **2006**, 1794-1801.

[40] C. Y. Gao, X. Qiao, Z. Y. Ma, Z. G. Wang, J. Lu, J. L. Tian, J. Y. Xu, S. P. Yan, *Dalton Trans.,* 41, **2012**, 12220-12232.

[41] A. Sharma, S. G. Schulman, Introduction of Fluorescence Spectroscopy, Wiley. New York, (1999) 58–59.

[42] S. Bi, D. Song, Y. Tian, X. Zhou, Z. Liu, H. Zhang, Spectrochimica. Acta. Part A: *Molecular and Biomolecular Spectroscopy*, 61, **2005**, 629-636.

[43] J. R. Lakowicz, Principles of Fluorescence Spectroscopy, Plenum Publishers, (1999).